HAL open science

In situ monitoring of alkanethiol self-assembly onto zinc selenide: the role of substrate pretreatment and its implication in bacterial attachment

Elena Yunda, Fabienne Quilès, David Horwat, Raúl Gago, Jaafar Ghanbaja, Halima Alem

To cite this version:

Elena Yunda, Fabienne Quilès, David Horwat, Raúl Gago, Jaafar Ghanbaja, et al.. In situ monitoring of alkanethiol self-assembly onto zinc selenide: the role of substrate pretreatment and its implication in bacterial attachment. Advanced Materials Interfaces, 2020, 7 (22), pp.2000848. 10.1002/admi.202000848 . hal-03021275

HAL Id: hal-03021275

https://hal.univ-lorraine.fr/hal-03021275v1

Submitted on 24 Nov 2020

HAL is a multi-disciplinary open access archive for the deposit and dissemination of scientific research documents, whether they are published or not. The documents may come from teaching and research institutions in France or abroad, or from public or private research centers.

L'archive ouverte pluridisciplinaire **HAL**, est destinée au dépôt et à la diffusion de documents scientifiques de niveau recherche, publiés ou non, émanant des établissements d'enseignement et de recherche français ou étrangers, des laboratoires publics ou privés.

Distributed under a Creative Commons Attribution 4.0 International License

Advanced Materials Interfaces, 2020, 7(22), 2000858. DOI:10.1002/admi.202000848

In situ monitoring of alkanethiol self-assembly onto zinc selenide: the role of substrate pretreatment and its implication in bacterial attachment

Elena Yunda, Fabienne Quilès, David Horwat, Raúl Gago, Jaafar Ghanbaja, and Halima Alem**

Dr E. Yunda, Dr F. Quilès
Université de Lorraine, CNRS, LCPME, F-54000 Nancy, France.
fabienne.quiles@univ-lorraine.fr

Dr E. Yunda, Prof. D. Horwat, Dr J. Ghanbaja, Dr H. Alem
Université de Lorraine, CNRS, IJL, F-54000 Nancy, France.
halima.alem@univ-lorraine.fr

Dr H. Alem
Institut Universitaire de France

Dr R. Gago
Instituto de Ciencia de Materiales de Madrid, Consejo Superior de Investigaciones Científicas, 28049 Madrid, Spain

Keywords: zinc selenide, surface functionalization, alkanethiol self-assembly, infrared spectroscopy, bacterial adhesion

Abstract

The interface between pioneer sessile bacteria and a supporting substrate can be probed *in situ* and at the molecular scale by infrared spectroscopy in the attenuated total reflection mode (ATR-FTIR). Here, a self-assembled monolayer (SAM) of amino-terminated alkanethiol is formed on the internal reflection element (IRE) composed of zinc selenide, and the attachment of model bacterium *Lactobacillus rhamnosus* GG (LGG) is subsequently studied. The impact of the beforehand surface preparation of the IRE on the SAM is studied on ZnSe substrates (i) cleaned by exposure to ozone/UV, (ii) acid cleaned or (iii) coated with a thin gold film. The surface properties of the obtained substrates are analyzed by atomic force and electron microscopies, and elastic ion backscattering spectrometry. The kinetics of the formation and the organization of the formed SAMs are strongly surface dependent, as evidenced with ATR-

FTIR. Acid-cleaned and gold-coated IREs are the least and most favorable substrates for alkanethiol SAM formation, respectively. Regardless of differences in SAM properties, the average degree of LGG attachment is similar on all functionalized substrates. The molecular organization of LGG cells, however, is substrate-dependent suggesting a possible effect of SAM organization on the bacteria-substrate interface.

1. Introduction

Biofilms are defined as communities of microorganisms embedded in a self-produced matrix of extracellular polymeric substances (EPS), and adherent to each other and/or a surface.[1] Biofilms are widespread on biological surfaces in the human body, in the environment, and on surfaces of medical and food equipment, water distribution systems and marine settings. The understanding of the formation of biofilms and, when suitable, the control of this process requires the understanding of the initial stages of their formation – bacterial adhesion. The latter is known to be influenced, among other things, by the surface properties of the support material.[2] In this regard, a large number of methods for detection and monitoring of bacterial adhesion on surfaces has been applied and developed.[3]

Among the methods used for the detection and the monitoring of the biofilm formation, infrared spectroscopy in the attenuated total reflection mode (ATR-FTIR) is a powerful tool for the comprehensive investigation of the process of bacterial attachment and early biofilm development (up to ≈1–2 μm thick). This method allows not only detecting biomass increase on the substrate in real time and *in situ*, but also determining the main biochemical components present in the biofilm without specific sample preparation, e.g. extraction and purification. The possibility to use ATR-FTIR spectroscopy to study sorption of pollutants by biofilms,[4–7] interaction of antimicrobials with biofilms,[8,9] as well as the role of EPS[5,10–13] and support surface[14–17] in biofilm formation has been illustrated. In particular, the works reporting the role

of support surface on bacterial adhesion were performed using internal reflection elements (IRE) transparent in the infrared and either coated with iron oxides[14,15] or plasma-treated.[16]

An advantageous route for surface modification is the self-assembly of alkanethiol molecules. In a simple protocol, this process enables obtaining a well-defined and controlled surface chemistry via covalently attached self-assembled monolayers (SAMs), which functionality can be tuned through the choice of the terminal group of the alkanethiol chain.[18] Indeed, SAMs have been successfully applied in studies of bacterial attachment using, for example, surface plasmon resonance spectroscopy[19,20] and optical microscopy[21] for *in situ* measurements on functionalized gold. It is noteworthy that SAMs formed on gold surfaces are the most common and well characterized systems for several reasons, including the inertness of gold, facility of the preparation of gold films, the use of gold in many characterization techniques and compatibility of gold with biological samples.[22] Few studies reported the feasibility to form alkanethiol SAMs on the infrared-transparent IRE composed of germanium[23–25] or zinc selenide (ZnSe).[17,26] The formation of SAMs on germanium is practically complicated due to the requirement of the surface pretreatment with highly corrosive and toxic hydrofluoric acid to remove surface oxides.[25] Conversely, the surface treatment of ZnSe can be performed prior to SAM adsorption using less corrosive acidic solutions, e.g. hydrogen peroxide and hydrochloric acid,[27] or by the exposure to ozone combined with UV radiation (ozone/UV).[26] Despite being of interest for ATR-FTIR studies with chemically modified surfaces, the properties of SAMs formed on ZnSe were scarcely addressed in literature[17,26].

Here, we decipher the differences in the process of alkanethiol self-assembly onto ZnSe IRE as a function of the surface pretreatment. Three methods to prepare the ZnSe surface prior to functionalization with the SAM were used: (i) exposure to ozone/UV, (ii) exposure to H_2O_2 followed by HCl aqueous solutions, and (iii) deposition of gold thin film onto ZnSe followed

by exposure to ozone/UV. The variations in the surface morphology and composition after these methods of preparation together with their correlation with the kinetics and surface coverage of alkanethiol SAMs are examined in this work. SAMs terminated with the $-NH_2$ functional group were chosen in this study as the amino group provides positive charge on the surface in physiological aqueous media. As most of bacteria are negatively charged in physiological conditions, it is a favorable case for the study of bacterial adhesion on the chemically modified substrate. We then explored the possibility to monitor the first steps of biofilm formation on the functionalized ZnSe using as a model bacterium *Lactobacillus rhamnosus* GG (LGG). The spectroscopic fingerprints of LGG recorded *in situ* and in real time revealed that the organization of the molecular groups in bacterial cells was different on gold-coated ZnSe, which could be associated with the highest density of SAM observed on this substrate. The degree of the LGG attachment was similar on ZnSe functionalized and pretreated by the three methods, indicating the versatility of the applied protocol for ZnSe surface optimization prior to SAM grafting. Collectively, the results of this study improve the understanding of alkanethiol self-assembly onto ZnSe and advance the potential of infrared spectroscopy in studying bacterial attachment and growth on chemically controlled surfaces.

2. Results and discussion

2.1. Characterization of ZnSe after surface pretreatments

Figure 1 shows the atomic force microscopy (AFM) topography images of ZnSe substrates after ozone/UV treatment, H_2O_2/HCl treatment, and gold coating. The resulting morphology of the substrates is characteristic of each procedure used for the substrate preparation. Long and straight scratches were observed on the surface after ozone/UV treatment (**Figure 1a**). These scratches are characteristic for ZnSe after the final polishing step in its manufacturing process [28] and lead to the roughness of the substrate of ≈5 nm (arithmetic average of surface heights measured across a surface, R_a). A drastic change in surface topography was noticed after

H_2O_2/HCl treatment. Indeed, the surface showed sphere-like features with the diameter of ~40 nm, which appeared homogeneously over the crystal surface (**Figure 1**b). After the acidic treatment, the roughness significantly increased to $R_a \approx 15$ nm. The cross-section of this sample observed by STEM also depicted nanosized hemispheric-like structures (~ 50 nm high) on the surface (**Figure 2a**). Of interest, these hemisphere-like features had nearly no zinc in their composition, and were very rich in selenium (**Figure 2a,b)**. Thus, the acidic treatment resulted in the preferential dissolution of Zn^{2+} ions from the surface resulting in a Se enriched nanostructures on the surface. The enrichment of ZnSe surface with selenium after H_2O_2/HCl etching was in accordance with previously reported works on ZnSe etching.[29–31] In the third case, when the ZnSe surface was coated with gold, the morphology reveals a homogeneous granular structure (**Figure 1**c). The gold grains had the width of ≈15 nm, as determined from the AFM measurements. The thickness of the gold coating was determined using ion elastic backscattering spectrometry (EBS) measurements (**Figure 3**). The area of the Au peak in the EBS spectra corresponds to the atomic areal density, and it was recalculated into the thickness given the known value of gold density. Thus, the equivalent thickness of the Au layer was estimated to be ≈2 nm. Similar morphologies of homogeneous few-nanometers thick gold films composed of nanosized grains were shown previously on silicone[32] and glass[33] substrates.

2.2. Organization of SAM on ZnSe and Au/ZnSe

Freshly prepared substrates were subjected to a solution of amino-terminated alkanethiol and the kinetics of the self-assembly was monitored *in situ* by ATR-FTIR spectroscopy (**Figure 4)**. It should be noted that the coating of the ATR crystal with a thin gold film can lead to the enhancement of the intensity of the infrared signal. This effect is called surface enhanced infrared absorption (SEIRA).[34] In this case, the orientation selection rules are those observed in infrared reflection-absorption spectroscopy (IRRAS). Namely, vibrational modes where the change in dipole moment is perpendicular to the surface appear strongly in the spectrum, whereas modes where the change in dipole moment is parallel to the surface appear very weak

or forbidden. The $\nu_{asym}CH_2/\nu_{sym}CH_2$ ratios calculated from the spectra of the SAMs on ZnSe and on ZnSe coated with gold were not significantly different (data not shown). Moreover, the SEIRA possible signal enhancement was found absent in measurements of phospholipidic supported bilayers onto Au/ZnSe with respect to bare ZnSe (figure S1 in supporting information). Therefore, we assume that difference in the signal intensity between alkanethiol SAMs on ZnSe or Au/ZnSe arises only from the difference in the surface density of the SAM on these two surfaces, and it is not associated with the possible effects of the thin metal film on the signal intensity. The increase of the integrated intensities of the νCH_2 infrared bands on all studied substrates was progressive for the first ~30 minutes and slowed down after, suggesting a two-stage process (**Figure 4**a). The mechanism, in which a rapid adsorption of alkanethiol molecules is followed by a slower process of the chain alignment was earlier suggested for SAMs obtained on other substrates.[18,23] In addition, the increase of the intensity of bands as a function of time can be reasoned by a progressive exchange of near-surface solvent with thiol molecules.[35] From the highest value of the integrated intensity of νCH_2 bands observed for the SAM on Au/ZnSe the coverage of the SAM was estimated to be the highest on this substrate. Here, it should be stressed that such result can be not only due to the higher affinity of S to Au with respect to Zn or Se, but also because of a lower roughness of the Au/ZnSe substrate that allows a more organized SAM. The low values of the integrated intensities observed on ZnSe after acidic treatment can thus be associated with the high substrate roughness, but also with the detrimental effect of selenium enrichment at the topmost surface. Indeed, Noble-Luginbuhl and Nuzzo hypothesized that thiols bind preferentially to Zn on ZnSe surfaces[26], and the results of the present work are in accordance with this hypothesis.

The experimental values shown in **Figure 4**a were fitted using equation 1 of Langmuir adsorption and rearrangement model ($r^2 \geq 0.95$):[36]

$$A = A_0\left(1 - A_{ads}e^{-t/\tau_{ads}} - (1 - A_{ads})e^{-t/\tau_{rea}}\right), \quad (1)$$

where A_0 is the limiting absorbance of a completely organized monolayer, A_{ads} is the adsorption coefficient, τ_{ads} is the rate constant of the adsorption phase, and τ_{rea} is the rate constant of the slow rearrangement phase. It must be noted that other equations based on Langmuir adsorption model can also be used to fit the kinetics of thiol adsorption.[23,37] Equation 1 was selected owing to its consideration of a slow adsorption phase, unlike other possible models. The results are gathered in **Table 1**. The value of τ_{ads} obtained on Au/ZnSe was ≈1.3 and 1.7 times smaller with respect to ZnSe (H_2O_2/HCl) and ZnSe (ozone/UV), respectively. Thus, the reaction occurred most rapidly on Au/ZnSe and was slower on ZnSe cleaned with ozone/UV and H_2O_2/HCl. The phase of the slow rearrangement was also affected by the substrate (τ_{rea}). On Au/ZnSe, the arrangement of alkanethiol molecules occurred ~8 and ~12 times faster than on ZnSe treated with ozone/UV and ZnSe treated with acid, respectively. It can also be noticed that the value of the limiting absorbance (A_0) was the highest on Au/ZnSe. The obtained values are overall in the same range as those found in the study of Lacour *et al.* describing the adsorption of alkanethiols onto gallium arsenide (A_{ads}=0.51, τ_{ads}=0.11, and τ_{rea}=2.62).[36]

The data on the kinetics of SAM formation and surface coverage were in good agreement with the organization of the SAM estimated from the position of νCH_2 bands (**Figure 4**b). Indeed, the lower wavenumber of $\nu_{asym}CH_2$ band of the SAM on Au/ZnSe compared to ZnSe suggests a lower number of conformational defects on the former surface.[38] The wavenumbers of $\nu_{asym}CH_2$ and $\nu_{sym}CH_2$ bands found for the SAM on ZnSe in this work were close to those found by Noble-Luginbuhl and Nuzzo for 1-dodecanethiol onto ZnSe, i.e. 2923 and 2853 cm^{-1}, respectively.[26] Based on the results reported in this section, it can be argued that SAM are better organized on Au/ZnSe substrates. We evaluate subsequently in the following the influence of the functionalized surface on bacteria attachment.

2.3. Attachment of bacteria on functionalized surfaces

After the functionalization with amino-terminated SAM, ZnSe and Au/ZnSe substrates were subjected to a flow of the bacterial suspension (at optical density 0.5 in physiological saline solution). As the selected SAM was terminated with amine groups, they were protonated under physiological conditions, providing an overall positive charge to the surfaces.[39] Bacteria are characterized with an overall negative charge of their cell wall[40] and hence, they can interact with the functionalized surfaces through electrostatic forces. The attachment of cells was monitored *in situ* and in real time by ATR-FTIR (**Figure 5**). The increase of the infrared bands in the spectra suggests the increase of the biomass on all studied surfaces. The bands were characteristic for bacteria,[41,42] showing namely the regions corresponding to proteins (1590–1490 cm^{-1}), nucleic acids and phospholipids (1270–1190 cm^{-1}) and polysaccharides combined with teichoic acids, nucleic acids and phospholipids (1190–956 cm^{-1}). Spectra of LGG were very similar on both SAM-NH_3^+ made on ZnSe without the gold coating (**Figure 5a,b**). Notably, they show the prominent peptido-polysaccharides from the cell wall as they were earlier observed[41] on bare ZnSe (i.e. without a SAM), mostly in region 1070-1000 cm^{-1}. The general feature of the bands absorbing between 1200 and 1000 cm^{-1} was different on SAM-NH_3^+ made on the gold-coated ZnSe (**Figure 5**c). The shoulders between 1070 and 950 cm^{-1} assigned to polysaccharides were less pronounced. The maximum height was at 1085 cm^{-1} (mostly assigned to the symmetric stretching of PO_2 groups[42]) and 1080 cm^{-1} for LGG on SAM-NH_3^+ on gold-coated ZnSe and SAM-NH_3^+ without the gold coating, respectively. In the case of SAM self-assembled on gold, phosphate groups were then more prominent. Considering these changes in spectral profile, ratios of the integrated intensities of the amide II band (1592-1486 cm^{-1}) and bands assigned to polysaccharides and nucleic acids (1189-956 cm^{-1}) were calculated for spectra recorded after 0.5 h and 2.5 h of LGG exposure to the surfaces (Table 2). On the surface pretreated by H_2O_2/HCl, all calculated ratios did not vary significantly. On the contrary, ratios

involving the amide II band were as ~1.3 lower from 0.5 h to 2.5 h of LGG exposure than on the two other prepared SAM-NH_3^+ (Table 2). These ratios also indicated that the PO_2 stretching modes absorbing at ~1230 and 1085 cm^{-1} are prominent in the spectra of bacteria attached on these both surfaces. Due to the short time of the experiment, bacteria did not change physiologically. Therefore, the differences between spectra were assigned to the changes in the interactions between the bacteria and the surface. These spectral features could indicate very strong electrostatic interactions of the phosphate groups from teichoic acids (anionic polymers) present at the surface of the Gram-positive bacteria[43] with the high density of NH_3^+ groups on both ozone/UV exposed bare ZnSe and gold-coated ZnSe surfaces with respect to the H_2O_2/HCl prepared surface.

The coverage of the functionalized substrates with LGG was similar on the three substrates, namely 26±6 % (ZnSe ozone/UV), 36±7 % (ZnSe H_2O_2/HCl), and 32±3 % (Au/ZnSe) (**Figure 5**). In fact, the retention of the bacteria after functionalization of ZnSe (ozone/UV) was 10-fold higher than without the functionalization, which confirms the influence of the functionalization step on the bacterial adhesion force (data not shown). Amide II band is considered as a good indicator of biomass present on the surface in ATR-FTIR spectroscopy. Despite similar bacterial coverages, it can be noticed that amide II band integrated intensities were 0.70, 0.82, and 1.23 for the spectra of LGG exposed to SAM-NH_3^+ on HCl/H_2O_2, ozone/UV and gold-coated ZnSe surfaces, respectively. Considering the size of the bacteria (~2 µm × 0.8 µm) and that the SEIRA effect can occur only within ~ 10 nm above the surface,[34] the latter phenomenon is negligible here, and thus, cannot explain the higher band intensities on SAM-NH_3^+ gold-coated surface. Another parameter affecting the intensity of the bands in ATR-FTIR spectra is the distance between the substrate and the bacterial cells.[44] Indeed, the evanescent wave at the origin of the signal decreases exponentially with the increase of the distance from the surface. Therefore, the higher Amide II band intensity on the gold-coated substrate may be associated with the higher number of NH_3^+ groups (**Figure 4a**) that lead to a closer contact of

the bacteria with the substrate, for example, through contracting their outer surface polymers enriched with carboxyl and phosphoryl groups.[44] The result showing similar coverage with bacteria regardless of the substrate indicates, however, that the number of amino groups on ZnSe without gold coating is still sufficient to maintain the cells attached. Bacteria were homogeneously distributed over the surfaces with a characteristic chain-like pattern, which was especially pronounced on ZnSe preliminarily treated with ozone/UV and on Au/ZnSe surfaces. Such cell-cell organization was previously observed for LGG and other lactobacilli, and is associated with the presence of surface appendages on the cell wall of this bacterium.[17,45–47] LGG cells appeared green after the staining, which suggested the integrity of their membrane, despite the presence of positive charges known as potential bactericides.[48,49] Possibly, this effect was attributed to the fact that LGG, like other Gram-positive bacteria, possess a thick peptidoglycan-rich layer on their cell wall that could act as a protective layer against detrimental electrostatic forces.[49,50]

3. Conclusion

This study reports the influence of surface pretreatments of ZnSe IRE on the processes of alkanethiol functionalization and subsequent bacterial attachment. The most drastic change in the morphology and the composition of ZnSe resulted from the acidic treatment. Indeed, the enrichment of the surface with selenium and the resulting higher roughness led to the lowest degree of functionalization with alkanethiol SAM. In contrast, a well ordered SAM with the highest surface coverage was formed on the gold-coated ZnSe substrate. On this substrate, the spectroscopic fingerprint of bacterial cells marked the enhanced interaction of the cell wall with the densely present NH_3^+ groups. All functionalized substrates, however, provided sufficient number of positive charges to maintain bacteria attached yet intact. These findings suggest that the three studied pretreatment protocols of ZnSe prior to alkanethiol functionalization are

suitable for the study of bacterial attachment, provided a possible impact of the modified IRE surface on bacterial spectral fingerprint is carefully considered.

4. Experimental Section

Materials: Trapezoidal ZnSe IREs (6.8 cm × 1 cm × 0.6 cm) and ZnSe disks (Ø 1.8 cm, thickness 1 mm) were purchased from Eurolabo and Crystran, respectively. 11-amino-1-undecanthiol hydrochloride (99%) was purchased from Sigma-Aldrich and used as received for formation of the SAM. Ethanol (RECTAPUR, 99.8%), isopropanol (SPECTROSOL) were purchased from Carlo Erba. H_2O_2 (30%, AnalaR NORMAPUR) and HCl (10% v/v in water) were purchased from VWR and Alpha Aesar, respectively. Sterile ultra-pure water (18.2 MΩ cm, Elga, Purelab Option-Q) was used to rinse the surface after functionalization of ZnSe with the SAM and after bacterial attachment.

Surface treatment of ZnSe prior to functionalization with the SAM: Prior to functionalization with the SAM, the ZnSe surface was prepared using one of the three methods: (i) exposure to ozone/UV (15 min) followed by the rinse with isopropanol and drying under N_2 flow;[26] (ii) dipping of the surface into H_2O_2 (10 %, 30 s), then into HCl (10 %, 1 min) (v/v) solutions, and final rinse with ethanol;[27] (iii) coating of ZnSe with gold, by magnetron sputtering as described below, and ozone/UV treatment (15 min), followed by the rinse with isopropanol and drying with N_2 flow. The cleaning and rinsing of the substrates were performed immediately before the mounting of the IRE in the infrared flow cells (Specac) and the start of the functionalization reaction.

Magnetron sputtering of gold onto ZnSe IRE: The deposition of thin films of gold on the surfaces of ZnSe IRE were performed using direct current magnetron sputtering of a gold target in presence of argon. The crystals were mounted on a rotating holder with the distance of 5 cm to the gold target (purity 99.99%). The argon flow in the deposition chamber was 50 cm^3 min^{-1}, whereas the working and base pressure values were 0.4 Pa and 10^{-4} Pa, respectively. The current applied to the target was 11 mA, resulting in a discharge voltage of 333 V (Pinnacle Plus DC

power supply, Advanced Energy). The sample holder was left at floating potential. The samples were etched with argon using radio frequency (RF) supply for 1 minute at 100 W and superimposed positive bias of -200 V, which was instantly followed by the deposition of gold for 1 minute. The obtained gold-coated ZnSe IRE (Au/ZnSe) were stored in ambient air until further use.

Characterization of ZnSe and Au/ZnSe surfaces: The characterization of ZnSe after surface pretreatment was performed on ZnSe disks. To study morphological features, atomic force microscopy (AFM) images were obtained using an Asylum Research MFP-3D Infinity™ apparatus equipped with a 100-µm close-loop scanner (Santa Barbara, USA). The images were recorded in the contact mode using a silicon nitride probe (MSCT, Bruker). The morphology and composition of ZnSe surface after treatment with H_2O_2/HCl was additionally studied using scanning transmission electron microscopy (STEM). A JEM–ARM 200F Cold FEG TEM/STEM instrument operating at 200 kV and equipped with a spherical aberration (Cs) probe was used for STEM analysis of the surface cross-section. This cross-section was prepared using focused ion beam technique (FIB). On the Au/ZnSe sample, the thickness of gold coating was verified using ion elastic backscattering spectrometry (EBS). The EBS measurements were performed with the 5 MV Cockroft–Walton tandetron (HVEE B.V., Amersfoort, The Netherlands) at Centro de Micro-Análisis de Materiales (CMAM) from Universidad Autónoma de Madrid. The incident energy of the He^+ projectiles was set at 4265 keV. As the measurements were performed in parallel with those reported in our previous work,[17] the energy value was selected to enhance the carbon signal at the surface. The incident angle of the beam was 50º, and a scattering angle was set at 170º for the detection of backscattered ions with a silicon detector. The experimental EBS spectra were analyzed by comparison with simulated spectra in SIMNRA software (Version 7.02). The results presented are representative from four measurements obtained on two different samples (two spots measured on each surface).

Functionalization of the IRE: The ZnSe trapezoid crystals were enclosed in a flow cell used for infrared spectroscopy as described elsewhere.[17,51] The infrared flow cell with ZnSe or Au/ZnSe IRE was filled with 2 mM ethanolic solution of 11-amino-1-undecanthiol hydrochloride and left for self-assembly reaction overnight. The surface of the crystal was subsequently rinsed inside the cell with ethanol and ultra-pure sterile water.

ATR-FTIR in situ monitoring of the SAM adsorption onto ZnSe and Au/ZnSe: A Bruker Tensor 27 FTIR spectrometer equipped with a KBr beam splitter and a deuterated triglycine sulfate (DTGS) thermal detector was used to record the spectra for monitoring of the self-assembly reaction. The spectrum of ethanol recorded just before the start of each experiment was used as a reference. Nitrogen gas was continuously purged throughout the infrared device for removal of the ethanol vapor, and therefore allowed avoiding its contribution in the infrared spectra.[52] The spectra were recorded every ≈1.5 minutes for the first 45 minutes and then every 20 minutes for a minimum of 15 hours. 100 scans were recorded to obtain each spectrum at a resolution of 4 cm^{-1}. The spectra were processed using OPUS 7.5 software (Bruker, Karlsruhe, Germany). All interferograms were Fourier processed using the Mertz phase correction mode and a Blackman-Harris three-term apodization function. ATR correction was not performed. Water vapor subtraction was performed and baseline was corrected at 3000 and 2820 cm^{-1}. The spectra presented are representative from three independent experiments.

Bacterial strain and culture conditions: *Lactobacillus rhamnosus* GG (LGG) is a probiotic bacterium, which properties are well described.[53,54] LGG ATCC 53103 strain used in this work was kindly provided by S. Lebeer (University of Antwerp, Belgium). LGG cultures were prepared in accordance with the previously described protocol.[41] Briefly, Man-Rogosa-Sharpe medium (ref. 288130, Difco) was used to prepare subcultures (20 mL, 24 hours) and cultures of bacteria (300 mL, 14 hours). Bacteria were grown in static conditions at 37°C.

Setup for bacterial attachment experiments: LGG suspensions were prepared from the above culture in 200 mL of physiological saline solution (NaCl 0.9 %) at an optical density of

0.50 ± 0.05 (cell density meter, model 40, Fisher Scientific, Illkirch, France). These suspensions were pumped around the infrared flow cell as previously described,[41] over the ZnSe surface functionalized with the SAM. After the flow cell was filled in with the bacterial suspension, the cells were let to adhere onto the crystal for 30 minutes in static conditions. The flow of the bacterial suspension was then carried out for 2 hours at 50 ml h^{-1} to obtain 2.5-hours-old biofilms.

ATR-FTIR in situ monitoring of LGG attachment on the functionalized IRE: The spectra were recorded using the same spectrometer as for the monitoring of alkanethiol adsorption, as detailed above. The reference spectrum was recorded immediately after filling in the cell with the bacterial suspension. The spectra were obtained from 100 scans every 10 minutes. Water vapor subtraction was performed and the baseline was corrected at 1800 and 900 cm^{-1}. The experiments were carried out at 21±1°C.

Epifluorescence microscopy: The average coverage of the surfaces with bacteria and the integrity of the bacterial membrane were estimated by staining the cells with the *Bac*Light™ kit (Molecular Probes, ref. L7012). The images were recorded with the × 10 objective of an Olympus BX51 microscope equipped with an Olympus XC50 camera. The *Bac*Light™ kit contains two dyes, Syto 9 and propidium iodide, which enable determination of the permeability state of the cell membrane. Green-fluorescent Syto 9 is able to penetrate into all cells, whereas red-fluorescent propidium iodide enters only the cells with compromised membranes making damaged bacteria appear red. The IRE with 2.5-hours-old biofilms were gently rinsed with ultrapure sterile water and bacteria were stained for 20 minutes in the dark at 21±1°C. The images (≈60) were recorded along the IRE surface, and processed with ImageJ software to calculate the percentage of the coverage of the surface with bacteria.

Supporting Information

Supporting Information is available from the Wiley Online Library or from the author.

Acknowledgements

This work was funded by Carnot Institute ICEEL. The authors are grateful to CC MEM of IJL and especially Sylvie Migot for the FIB preparation of the samples for STEM experiments. We also thank the Spectroscopy and Microscopy Service Facility (SMI) of LCPME (Université de Lorraine-CNRS – http://www.lcpme.cnr-nancy.fr) where infrared experiments were performed.

Received: ((will be filled in by the editorial staff))
Revised: ((will be filled in by the editorial staff))
Published online: ((will be filled in by the editorial staff))

References

[1] H.-C. Flemming, J. Wingender, U. Szewzyk, P. Steinberg, S. A. Rice, S. Kjelleberg, *Nature Reviews Microbiology* **2016**, *14*, 563.
[2] H. H. Tuson, D. B. Weibel, *Soft Matter* **2013**, *9*, 4368.
[3] G. Schaule, T. Griebe, H.-C. Flemming, in *Flemming, H.C., Szewzyk, U., Griebe, T. Biofilms*, CRC Press, Boca Raton, **2000**.
[4] L. Zhou, F. Dong, H. Li, T. Huo, P. Wang, M. Liu, G. Yang, W. Zhang, W. Hu, X. Nie, H. He, B. Li, R. L. Frost, *Chemical Engineering Journal* **2019**, *359*, 393.
[5] S. Kumari, N. Mangwani, S. Das, *Spectrochimica Acta Part A: Molecular and Biomolecular Spectroscopy* **2017**, *173*, 655.
[6] J.-H. Huang, E. J. Elzinga, Y. Brechbuehl, A. Voegelin, R. Kretzschmar, *Environ. Sci. Technol.* **2011**, *45*, 2804.
[7] J. Schmitt, D. Nivens, D. C. White, H.-C. Flemming, *Water Science and Technology* **1995**, *32*, 149.
[8] P. A. Suci, G. G. Geesey, B. J. Tyler, *Journal of Microbiological Methods* **2001**, *46*, 193.
[9] F. Quilès, S. Saadi, G. Francius, J. Bacharouche, F. Humbert, *Biochimica et Biophysica Acta (BBA) - Biomembranes* **2016**, *1858*, 75.
[10] J. Hou, D. H. Veeregowda, B. van de Belt-Gritter, H. J. Busscher, H. C. van der Mei, *Applied and Environmental Microbiology* **2018**, *84*, DOI 10.1128/AEM.01516-17.
[11] D. E. Nivens, D. E. Ohman, J. Williams, M. J. Franklin, *J Bacteriol* **2001**, *183*, 1047.
[12] R. M. Donlan, J. A. Piede, C. D. Heyes, L. Sanii, R. Murga, P. Edmonds, I. El-Sayed, M. A. El-Sayed, *Applied and Environmental Microbiology* **2004**, *70*, 4980.
[13] G. S. Lorite, A. A. de Souza, D. Neubauer, B. Mizaikoff, C. Kranz, M. A. Cotta, *Colloids and Surfaces B: Biointerfaces* **2013**, *102*, 519.
[14] J. J. Ojeda, M. E. Romero-Gonzalez, H. M. Pouran, S. A. Banwart, *Mineralogical Magazine* **2008**, *72*, 101.
[15] S. J. Parikh, F. N. D. Mukome, X. Zhang, *Colloids and Surfaces B: Biointerfaces* **2014**, *119*, 38.
[16] M. Pousti, J. Greener, *Surface Science* **2018**, *676*, 56.
[17] E. Yunda, H. Alem, G. Francius, R. Gago, F. Quilès, *ACS Appl. Mater. Interfaces* **2020**, *12*, 14933.
[18] C. D. Bain, E. B. Troughton, Y. T. Tao, J. Evall, G. M. Whitesides, R. G. Nuzzo, *J. Am. Chem. Soc.* **1989**, *111*, 321.
[19] J.-S. Guo, P. Zhang, Y.-P. Chen, Y. Shen, X. Hu, P. Yan, J.-X. Yang, F. Fang, C. Li, X. Gao, G.-X. Wang, *Chemical Engineering Journal* **2015**, *279*, 516.

[20] A. Pranzetti, S. Salaün, S. Mieszkin, M. E. Callow, J. A. Callow, J. A. Preece, P. M. Mendes, *Advanced Functional Materials* **2012**, *22*, 3672.
[21] K. M. Wiencek, M. Fletcher, *Biofouling* **1997**, *11*, 293.
[22] J. C. Love, L. A. Estroff, J. K. Kriebel, R. G. Nuzzo, G. M. Whitesides, *Chem. Rev.* **2005**, *105*, 1103.
[23] M. R. Kosuri, R. Cone, Q. Li, S. M. Han, B. C. Bunker, T. M. Mayer, *Langmuir* **2004**, *20*, 835.
[24] S. M. Han, W. R. Ashurst, C. Carraro, R. Maboudian, *J. Am. Chem. Soc.* **2001**, *123*, 2422.
[25] M. Lommel, E. Mankel, B. Kolbesen, *ECS Transactions* **2008**, *11*, 83.
[26] A. R. Noble-Luginbuhl, R. G. Nuzzo, *Langmuir* **2001**, *17*, 3937.
[27] C. S. Riccardi, D. W. Hess, B. Mizaikoff, *Analyst* **2011**, *136*, 4906.
[28] *The Crystran Handbook of Infra-Red and Ultra-Violet Optical Materials*, Crystran Ltd, **2016**.
[29] T. F. McGee, H. J. Cornelissen, *Applied Surface Science* **1989**, *35*, 371.
[30] A. Kita, M. Ozawa, C. D. Gutleben, *Applied Surface Science* **1996**, *100*, 652.
[31] J. Zhao, M. H. Na, E. H. Lee, H. C. Chang, J. A. Gardella, H. Luo, *Journal of Vacuum Science & Technology B: Microelectronics and Nanometer Structures Processing, Measurement, and Phenomena* **1998**, *16*, 3048.
[32] A. Klimovskaya, A. Sarikov, Y. Pedchenko, A. Voroshchenko, O. Lytvyn, A. Stadnik, *Nanoscale Res Lett* **2011**, *6*, 151.
[33] E. N. Aybeke, Y. Lacroute, C. Elie-Caille, A. Bouhelier, E. Bourillot, E. Lesniewska, *Nanotechnology* **2015**, *26*, 245302.
[34] P. R. Griffiths, in *Spectroscopic Properties of Inorganic and Organometallic Compounds: Techniques, Materials and Applications, Volume 44*, The Royal Society Of Chemistry, **2013**, pp. 95–122.
[35] C. Vericat, M. E. Vela, G. Benitez, P. Carro, R. C. Salvarezza, *Chem. Soc. Rev.* **2010**, *39*, 1805.
[36] V. Lacour, K. Moumanis, W. M. Hassen, C. Elie-Caille, T. Leblois, J. J. Dubowski, *Langmuir* **2019**, *35*, 4415.
[37] S. S. Cheng, D. A. Scherson, C. N. Sukenik, *J. Am. Chem. Soc.* **1992**, *114*, 5436.
[38] M. D. Porter, T. B. Bright, D. L. Allara, C. E. D. Chidsey, *J. Am. Chem. Soc.* **1987**, *109*, 3559.
[39] K. P. Fears, S. E. Creager, R. A. Latour, *Langmuir* **2008**, *24*, 837.
[40] A. T. Poortinga, R. Bos, W. Norde, H. J. Busscher, *Surface Science Reports* **2002**, *47*, 1.
[41] E. Yunda, F. Quilès, *Biofouling* **2019**, *35*, 494.
[42] B. (Barbara H.) Stuart, *Infrared Spectroscopy : Fundamentals and Applications*, Chichester, West Sussex, England ; Hoboken, NJ : J. Wiley, [2004] ©2004, **2004**.
[43] T. Shirashi, S. Yokota, S. Fukiya, A. Yokota, *Bioscience of Microbiota, Food and Health* **2016**, *35*, 147.
[44] S.-Y. Kang, P. J. Bremer, K.-W. Kim, A. J. McQuillan, *Langmuir* **2006**, *22*, 286.
[45] P. Tripathi, A. Beaussart, G. Andre, T. Rolain, S. Lebeer, J. Vanderleyden, P. Hols, Y. F. Dufrêne, *Micron* **2012**, *43*, 1323.
[46] M. Jarosz, J. Grudzień, K. Kamiński, K. Gawlak, K. Wolski, M. Nowakowska, G. D. Sulka, *Electrochimica Acta* **2019**, *296*, 999.
[47] M. C. Leccese Terraf, M. S. Juárez Tomás, L. Rault, Y. Le Loir, S. Even, M. E. F. Nader-Macías, *Archives of Microbiology* **2016**, *198*, 689.
[48] C. Chen, T. Petterson, J. Illergård, M. Ek, L. Wågberg, *Biomacromolecules* **2019**, *20*, 2075.
[49] A. Terada, A. Yuasa, T. Kushimoto, S. Tsuneda, A. Katakai, M. Tamada, *Microbiology* **2006**, *152*, 3575.

[50] B. Gottenbos, D. W. Grijpma, H. C. van der Mei, J. Feijen, H. J. Busscher, *Journal of Antimicrobial Chemotherapy* **2001**, *48*, 7.
[51] A. Delille, F. Quilès, F. Humbert, *Applied and Environmental Microbiology* **2007**, *73*, 5782.
[52] E. K. Plyler, *Journal of Research of the National Bureau of Standards* **1952**, *48*, Research Paper: 2314.
[53] S. Doron, D. R. Snydman, S. L. Gorbach, *Gastroenterol Clin North Am.* **2005**, *34*, 483.
[54] M. E. Segers, S. Lebeer, *Microbial Cell Factories* **2014**, *13*, S7.

Figure 1. AFM topography images of ZnSe substrates after ozone/UV treatment (a), H_2O_2/HCl treatment (b), and gold coating (c)

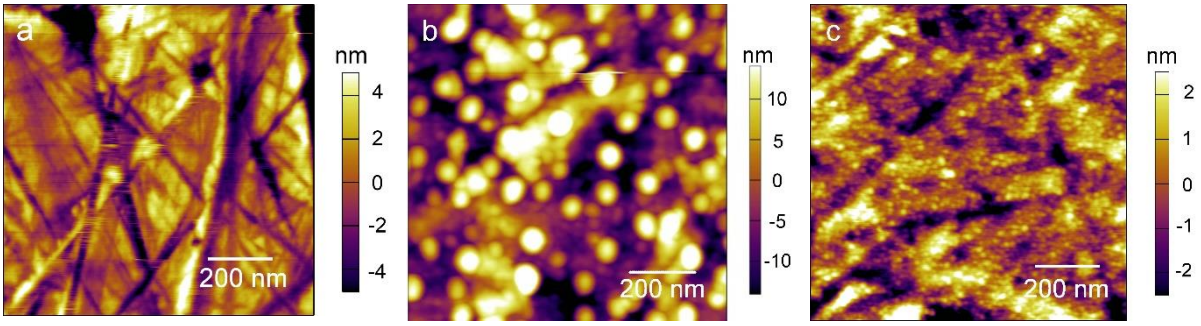

Figure 2. STEM analysis of ZnSe after H_2O_2/HCl treatment: SEM photograph of the surface cross-section (a) and EDS maps of the surface cross-section for Zn (b) and Se (c) elements

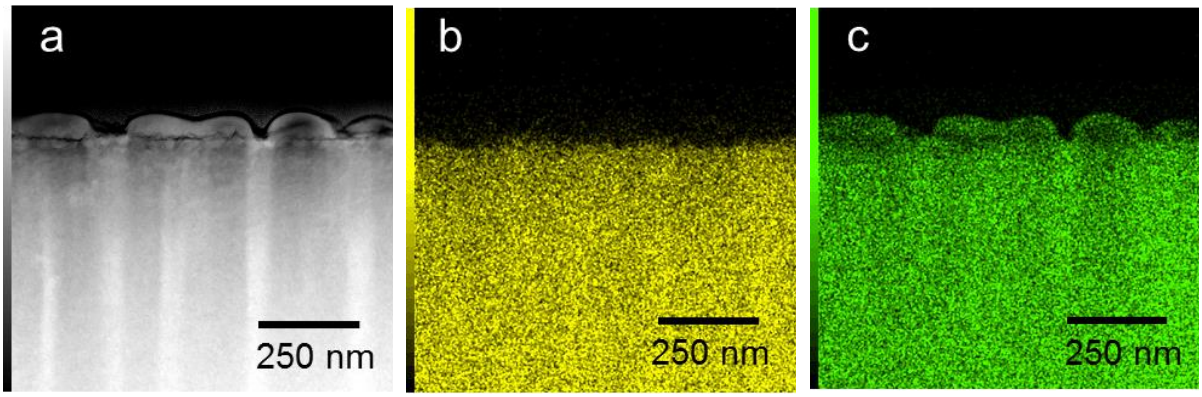

Figure 3. Ion elastic backscattering spectrum showing experimental and simulated curves for the yield of Zn, Se and Au counts on Au-coated ZnSe.

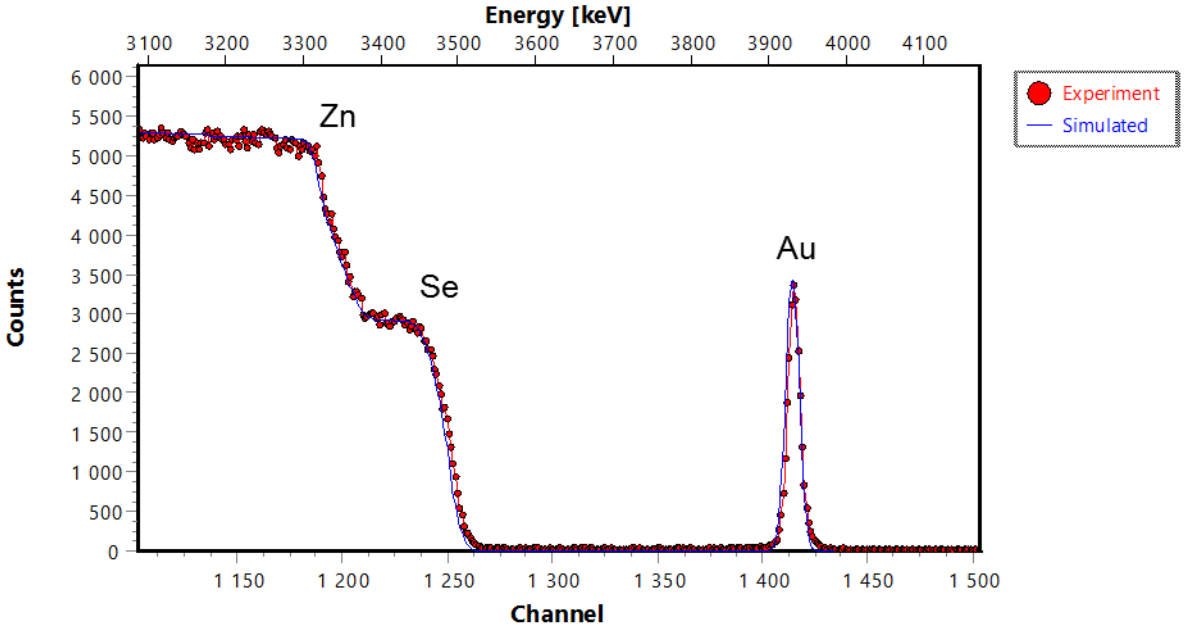

Figure 4. (a) Time evolution of the integrated intensities of νCH_2 symmetric and antisymmetric stretching bands (2964–2820 cm^{-1}) of amino-terminated alkanethiol adsorbed on the pretreated ZnSe substrates. Standard deviations were obtained from three independent experiments. (b) Corresponding spectra obtained on these substrates after ~2 min (- - -) and 15 hours (—) of the reaction (the spectrum of ethanol is the reference). The shift of the νCH_{2asym} band to a lower ν suggests the increase of ordering in SAMs over time. a.u.: arbitrary units.

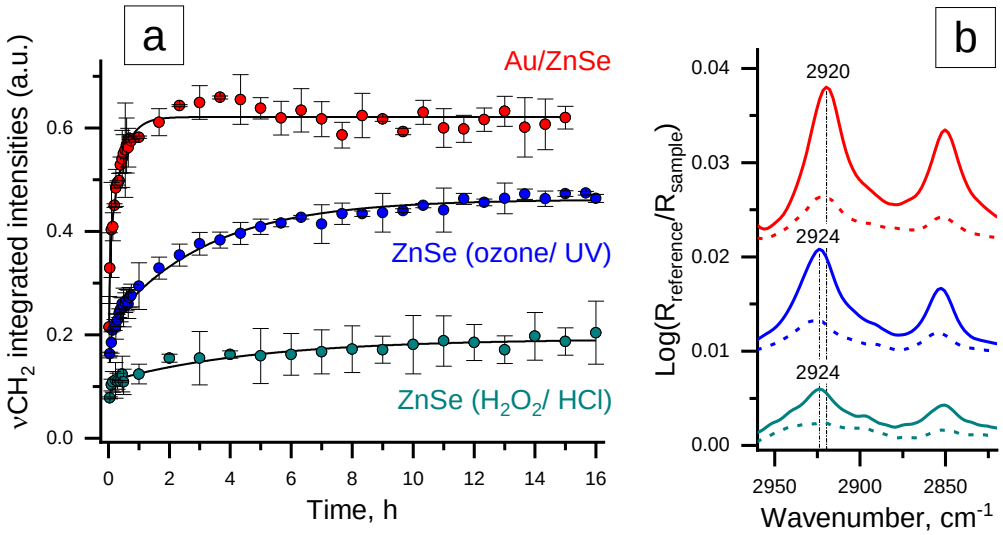

Figure 5. Time-evolution of the infrared spectra in attenuated total reflection mode during the LGG exposure on the substrates functionalized with amino-terminated SAM ((left column, offsets are used for clarity and main assignments are provided), and corresponding epifluorescence images of the bacteria on the substrates after 2.5 h of exposure (right column, scale bar – 200 µm).

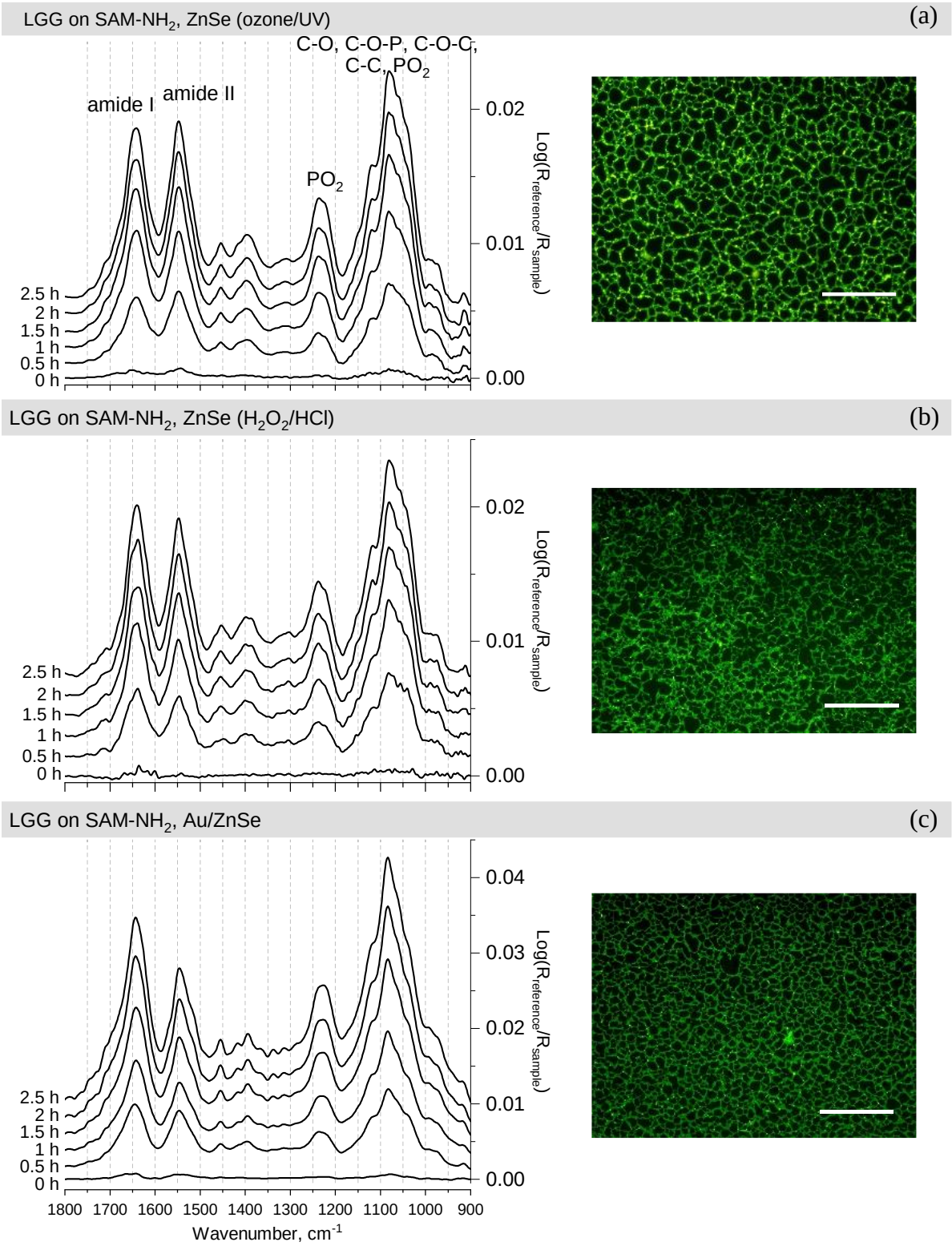

Table 1. Parameters derived from the fitting of adsorption curves of SAM-NH_2 on the three different substrates.

	Au/ZnSe	ZnSe (ozone/UV)	ZnSe (H_2O_2/HCl)
A_0	0.62	0.46	0.19
A_{ads}	0.55	0.47	0.57
τ_{ads}	0.03	0.05	0.04
τ_{rea}	0.39	3.16	4.84

Table 2. Ratios of integrated intensities calculated from amide II (1592 – 1486 cm^{-1}), phosphate antisymmetric stretching (PO_2, 1271 - 1188 cm^{-1}) and nucleic acids + phospholipids + polysaccharides (NA+PL+PS, 1189 – 956 cm^{-1}) after 0.5 and 2.5 hours of exposure of LGG on the three different substrates.

Pretreatment of the surface for SAM-NH_2	Amide II/PO_2		Amide II/AN+PL+PS		PO_2/AN+PL+PS	
	0.5 h	2.5 h	0.5 h	2.5 h	0.5 h	2.5 h
ZnSe - H_2O_2/HCl	1.76	1.71	0.39	0.40	0.22	0.23
ZnSe - ozone/UV	2.28	1.82	0.51	0.43	0.21	0.24
Au/ZnSe	1.64	1.18	0.42	0.31	0.25	0.26